DRUG METABOLISM & DISPOSITION

Human UDP-Glucuronosyltransferase (UGT) 2B10: Validation of Cotinine as a Selective Probe Substrate, Inhibition by UGT Enzyme-Selective Inhibitors and Antidepressant and Antipsychotic Drugs, and Structural Determinants of Enzyme Inhibition[S]

Attarat Pattanawongsa, Pramod C. Nair, Andrew Rowland, and John O. Miners

Department of Clinical Pharmacology (A.P., P.C.N., A.R., J.O.M.) and Flinders Centre for Innovation in Cancer (A.R., P.C.N., J.O.M.), Flinders University School of Medicine, Adelaide, Australia

Received November 2, 2015; accepted December 14, 2015

ABSTRACT

Although there is evidence for an important role of UGT2B10 in the N-glucuronidation of drugs and other xenobiotics, the inhibitor selectivity of this enzyme is poorly understood. This study sought primarily to characterize the inhibition selectivity of UGT2B10 by UDP-glucuronosyltransferase (UGT) enzyme-selective inhibitors used for reaction phenotyping, and 34 antidepressant and antipsychotic drugs that contain an amine functional group. Initial studies demonstrated that cotinine is a highly selective substrate of human liver microsomal UGT2B10. The kinetics of cotinine N-glucuronidation by recombinant UGT and human liver microsomes (± bovine serum albumin) were consistent with the involvement of a single enzyme. Of the UGT enzyme-selective inhibitors employed for reaction pheno-typing, only the UGT2B4/7 inhibitor fluconazole reduced recombinant UGT2B10 activity to an appreciable extent. The majority of antidepressant and antipsychotic drugs screened for effects on UGT2B10 inhibited enzyme activity with IC$_{50}$ values <100 μM. The most potent inhibition was observed with the tricyclic antidepressants amitriptyline and doxepin and the tetracyclic antidepressant mianserin, and the structurally related compounds desloratadine and loratadine. Molecular modeling using a ligand-based approach indicated that hydrophobic and charge interactions are involved in inhibitor binding, whereas spatial features influence the potency of UGT2B10 inhibition. Respective mean K$_{i,u}$ (± S.D.) values for amitriptyline, doxepin, and mianserin inhibition of human liver microsomal UGT2B10 were 0.61 ± 0.05, 0.95 ± 0.18, and 0.43 ± 0.01 μM. In vitro–in vivo extrapolation indicates that these drugs may perpetrate inhibitory drug-drug interactions when coadministered with compounds that are cleared predominantly by UGT2B10.

Introduction

Enzymes of the UDP-glucuronosyltransferase (UGT) superfamily catalyze the covalent linkage (conjugation) of glucuronic acid, which is derived from the cofactor UDP-glucuronic acid (UDP-GlcUA), to a typically lipophilic substrate containing a nucleophilic acceptor functional group. Functional groups that are glucuronidated include hydroxyl (aliphatic and phenolic), carboxylic acids, amines (primary, secondary, tertiary, and aromatic), and thiols. Consistent with the ability of UGTs to metabolize compounds containing these commonly occurring functional groups, glucuronidation serves as an elimination and detoxification mechanism for drugs from almost all therapeutic classes, nondrug xenobiotics, endogenous compounds, and the products of oxidative metabolism (Miners and Mackenzie, 1991; Miners et al., 2004; Kiang et al., 2005). Twenty-two human UGT proteins have been identified to date (Mackenzie et al., 2005). Nineteen of these, classified in the UGT 1A, 2A, and 2B subfamilies, primarily use UDP-GlcUA as cofactor.

Available evidence indicates that the individual UGT enzymes exhibit distinct but sometimes overlapping substrate and inhibitor selectivities (Miners et al., 2004, 2010a; Rowland et al., 2013). However, data are lacking for several UGTs, especially with respect to inhibitor profiles.

UGT2B10 was cloned initially in this laboratory and demonstrated to lack activity toward hydroxylated xenobiotics and steroids (Jin et al., 1993). The inability of UGT2B10 to catalyze the O-glucuronidation of these compounds was subsequently shown to arise from substitution of the near conserved His, present in the N terminus putative substrate binding domain of all UGT family 1 and 2 enzymes except UGT1A4 and UGT2B10, with Leu (Kerdpin et al., 2009). Substitution of Leu[34] of UGT2B10 with His, which functions as the catalytic base in O-glucuronidation reactions, generated an enzyme that metabolized the phenols 4-methylumbelliferone (4MU) and 1-naphthol.

Although initially considered an orphan enzyme, more recent studies have shown that UGT2B10, like UGT1A4, catalyzes the N-glucuronidation of a number of xenobiotics that incorporate an aliphatic tertiary amine or aromatic N-heterocyclic group (Kaivosaari et al., 2011). Known substrates are nicotine and its oxidation product cotinine (Chen et al., 2007; Kaivosaari et al., 2007); desloratadine (Kazmi et al., 2015a); medetomidine (Kaivosaari et al., 2008); the tricyclic antidepressants

ABBREVIATIONS: AUC, area under the plasma drug concentration–time curve; BSA, bovine serum albumin; DDI, drug-drug interaction; fu, fraction unbound in plasma; HCl, hydrochloride; HLM, human liver microsomes; HPLC, high-performance liquid chromatography; MAOI, monoamine oxidase inhibitor; 4MU, 4-methylumbelliferone; RED, rapid equilibrium dialysis; SNRI, serotonin and noradrenaline reuptake inhibitor; SSRI, selective serotonin reuptake inhibitor; TCA, tricyclic antidepressant; UDP-GlcUA, UDP-glucuronic acid; UGT, UDP-glucuronosyltransferase.

(TCAs) amitriptyline, clomipramine, imipramine, and trimipramine (Chen et al., 2007; Zhou et al., 2010; Kato et al., 2013); several tobacco-specific nitrosamines (Chen et al., 2008); RO5263397 (Fowler et al., 2015); and miscellaneous drugs that include diphenhydramine, ketoconazole, ketotifen, midazolam, olanzapine, pizotifen, and tamoxifen (Erickson-Ridout et al., 2011; Kato et al., 2013). Consistent with the known selectivity of UGT1A4 for N-glucuronidation (Kubota et al., 2007), most, if not all, UGT2B10 substrates are additionally glucuronidated by UGT1A4 and biphasic kinetics are frequently observed when human liver microsomes (HLM) are used as the enzyme source (Kaivosaari et al., 2011; Kato et al., 2013). However, available evidence indicates that UGT2B10 is the high-affinity enzyme involved in most reactions.

The UGT2B10 substrates desloratadine and nicotine further act as inhibitors of this enzyme. In particular, desloratadine has been reported to be a relatively selective and potent competitive inhibitor of UGT2B10, with a K_i of 1.3 μM (Kazmi et al., 2015b). Nicotine has also been employed as an inhibitor of UGT2B10 in vitro, although the UGT enzyme inhibition selectivity of this compound is incompletely characterized (Zhou et al., 2010). A large number of clinically used drugs contain an aliphatic amine or aromatic N-heterocyclic group. Notable in this regard are antidepressants [TCAs, selective serotonin reuptake inhibitors (SSRIs), serotonin and noradrenaline reuptake inhibitors (SNRIs), tetracyclic antidepressants, and monoamine oxidase inhibitors (MAOIs)] and antipsychotics (both typical and atypical). Indeed, the majority of drugs in these classes are either tertiary or secondary aliphatic amines. Despite their widespread clinical use, however, the potential inhibition of UGT2B10 by these compounds has not been explored in a systematic manner. Furthermore, knowledge of the effects of UGT enzyme-selective inhibitors employed for reaction phenotyping in vitro on UGT2B10 activity is similarly lacking (Miners et al., 2010a).

Thus, the aims of the present study were to confirm the UGT enzyme selectivity of cotinine as a UGT2B10 substrate and desloratadine and nicotine as UGT2B10 inhibitors; investigate the potential inhibition of UGT2B10 by currently used UGT enzyme-selective inhibitors employed for reaction phenotyping; and characterize the inhibition of UGT2B10 by 34 amine (primary, secondary, and tertiary) containing antidepressants and antipsychotics from various classes (TCAs, SSRIs, SNRIs, MAOIs, and typical and atypical antipsychotics). Data generated from these studies were employed to identify the structural features of compounds required for potent inhibition of UGT2B10 and to provide insights into potential drug-drug interactions (DDIs) arising from inhibition of this enzyme.

Materials and Methods

Materials

Alamethicin (from *Trichoderma viride*), amitriptyline hydrochloride (HCl), aripiprazole, bovine serum albumin (BSA; essentially fatty acid free), chlorpromazine HCl, clomipramine HCl, clozapine, codeine, S-(-)-cotinine, desipramine HCl, desvenlafaxine HCl, diclofenac (sodium salt), doxepin HCl, fluphenazine HCl, fluvoxamine maleate, hecogenin, imipramine HCl, 4MU, 4-methylumbelliferone glucuronide, mirtazapine, S-(-)-nicotine, niflumic acid, norclomipramine HCl, nortriptyline HCl, perphenazine, phenylbutazone, protriptyline HCl, selegiline HCl, thioridazine HCl, tranylcypromine HCl, trimipramine HCl, and UDP-GlcUA (trisodium salt) were purchased from Sigma-Aldrich (Sydney, Australia); codeine 6-O-glucuronide, cotinine N-β-D-glucuronide, citalopram hydrobromide, desloratadine, fluoxetine HCl, loratadine, olanzapine, phenelzine sulfate, quetiapine hemifumarate, and sertraline HCl from Toronto Research Chemicals (North York, ON, Canada); duloxetine HCl from Selleck Chemicals (Houston, TX); and haloperidol, paroxetine, and venlafaxine HCl from Cayman Chemicals (Ann Arbor, MI). Didesmethylimipramine HCl was a gift of Ciba-Geigy (Basel, Switzerland); desmethylnortriptyline HCl from Roche (Basel, Switzerland);

fluconazole from Pfizer Australia (Sydney, Australia); lamotrigine and lamotrigine N2-glucuronide from the Wellcome Research Laboratories (Beckenham, UK); ketoconazole and itraconazole from Janssen Research Foundation (New York, NY); mianserin HCl from Akzo Pharmaceutical Division (Arnhem, The Netherlands); and loxapine from Alexza Pharmaceuticals (Mountain View, CA). Supersomes expressing UGT2B4, UGT2B7, UGT2B10, UGT2B15, and UGT2B17 and pooled HLM (150 donor pool; equal number of males and females) were purchased from BD Biosciences (San Jose, CA). Rapid equilibrium dialysis (RED) inserts and base plates were purchased from Thermo Scientific (Rockford, IL). Solvents and other reagents used were of analytical reagent grade.

Methods

HLM and Recombinant Human UGTs. Approval for the use of human liver tissue for in vitro drug metabolism studies was obtained from the Southern Adelaide Clinical Research Ethics Committee. HLM were activated by preincubation with the pore-forming agent alamethicin (50 μg/mg microsomal protein) prior to use in incubations according to Boase and Miners (2002). Human UGT 1A1, 1A3, 1A4, 1A6, 1A7, 1A8, 1A9, and 1A10 cDNAs were stably expressed in a human embryonic kidney cell line (HEK293T), according to Uchaipichat et al. (2004). Cells expressing the individual UGTs were lysed by sonication using a Vibra Cell VCX 130 Ultrasonics Processor (Sonics and Materials, Newtown, CT). The lysates were centrifuged at 12,000g for 1 minute at 4°C, and the supernatant fractions were separated and stored in phosphate buffer (0.1 M, pH 7.4) at −80°C until use. Given the lower expression of UGT 2B4, 2B7, 2B10, 2B15, and 2B17 in HEK293 cells, Supersomes expressing these proteins were used for activity and inhibition studies.

Cotinine N-Glucuronidation by Recombinant UGTs and HLM. Thirteen recombinant human UGTs were screened for cotinine N-glucuronide formation, as follows: UGT 1A1, 1A3, 1A4, 1A6, 1A7, 1A8, 1A9, 1A10, 2B4, 2B7, 2B10, 2B15, and 2B17. Incubations (100 μl total volume) contained cotinine (0.25, 1, and 5 mM), Supersome or HEK293 lysate protein (1 mg/ml), 0.1 M phosphate buffer (pH 7.4), and 4 mM MgCl$_2$. The incubation mixtures were preincubated at 37°C for 5 minutes, and then reactions were initiated by the addition of 5 mM UDP-GlcUA. Incubations were performed at 37°C for 120 minutes, after which time reactions were terminated by the addition of 11.6 M HClO$_4$ (1 μl). Samples were cooled on ice for 10 minutes and then centrifuged at 5000g, 4°C, for 10 minutes. An aliquot was injected onto the high-performance liquid chromatography (HPLC) column (see below). For the kinetic characterization of cotinine N-glucuronidation by recombinant UGT2B10 and HLM, incubations were conducted as described above for recombinant UGTs and contained either UGT2B10-expressing Supersomes (1 mg/ml) or HLM (0.5 mg/ml). The kinetics of cotinine N-glucuronidation were characterized in the absence and presence of BSA (1% w/v). Incubations containing BSA were terminated by the addition of 3 μl 11.6 M HClO$_4$.

Quantification of Cotinine N-Glucuronide Formation. Cotinine N-glucuronide formation was measured using an Agilent 1200 series HPLC system (Agilent Technologies, Sydney, Australia) fitted with a Zorbax Eclipse XBD-C8, 4.6 × 150 mm, 5 μm (Agilent Technologies). Cotinine N-glucuronide was eluted by isocratic elution with a 96:4 mixture of mobile phases A (4 mM 1-octanesulfonic acid adjusted to pH 2.7 with 11.6 M HClO$_4$) and B (acetonitrile) at a flow rate of 1 ml/min. Column eluent was monitored at a wavelength of 254 nm. The retention times of cotinine N-glucuronide and cotinine were 7 and 43 minutes, respectively. Cotinine N-glucuronide was quantified by reference to a calibration curve prepared using an authentic standard. Calibration curve concentration ranges were 1–5 μM and 1–25 μM with UGT2B10 and HLM as the respective enzyme sources.

Inhibition of Recombinant Human UGT2B10 Activity by Antidepressants, Antipsychotics, and Other Compounds. The inhibition of recombinant human UGT2B10 enzyme activity was determined for 43 compounds (see *Results*). Effects on UGT2B10 activity were investigated at four inhibitor concentrations (1, 10, 100, and 500 μM), except for fluconazole (1, 2.5, 5, and 10 mM), hecogenin (1, 10, 50, and 100 μM), itraconazole (1, 10, 50, and 100 μM), ketoconazole (1, 10, 100, and 200 μM), and niflumic acid (1, 10, 100, and 200 μM). Stock solutions of the antidepressant and antipsychotic drugs available as salts (see *Materials and Methods*) were prepared in water. Stock solutions of all other inhibitors were prepared in dimethylsulfoxide, with the following exceptions: desloratadine and nicotine stock solutions were prepared in ethanol, whereas hecogenin was dissolved in methanol. The final concentration of solvent present in

incubation mixtures was 1% (v/v). The inhibition studies were performed at a cotinine concentration of 2.8 mM, which corresponds to the apparent K_m for cotinine N-glucuronidation by recombinant UGT2B10 (see *Results*).

Inhibition of Recombinant Human UGT Enzyme Activities by Desloratadine and Nicotine. In addition to effects on UGT2B10, desloratadine and nicotine (1, 10, 100, and 500 μM) were screened for inhibition of the UGT1A and UGT2B subfamily enzymes UGT 1A1, 1A3, 1A4, 1A6, 1A7, 1A8, 1A9, 1A10, 2B4, 2B7, 2B15, and 2B17. Effects on all enzymes except UGT1A4 and UGT2B4 were determined using the nonselective substrate 4MU. The 4MU concentration used in incubations corresponded to the published apparent K_m or S_{50} of each enzyme, whereas protein concentrations and incubation time varied for each enzyme, as described by Uchaipichat et al. (2004). The 4MU glucuronide formation was quantified according to Lewis et al. (2007). Inhibition of UGT1A4 by desloratadine and nicotine was assessed with lamotrigine as the probe substrate following the method of Rowland et al. (2006), whereas effects on UGT2B4 activity were determined with codeine as the substrate, as described by Raungrut et al. (2010). Concentrations of lamotrigine and codeine used in the UGT1A4 and UGT2B4 inhibition-screening studies corresponded to the respective K_m values for each substrate/pair: 1.5 mM for lamotrigine/UGT1A4 and 2.0 mM for codeine/UGT2B4. Positive control inhibitors were used in all inhibition screening experiments, as described in Pattanawongsa et al. (2015). The magnitude of inhibition of each positive control inhibitor (data not shown) was as expected from previous studies in this laboratory (Uchaipichat et al., 2004, 2006a, 2006b; Raungrut et al., 2010; Miners et al., 2011).

Inhibition of Human Liver Microsomal Cotinine N-Glucuronidation by Hecogenin and Desloratadine. The relative contributions of UGT1A4 and UGT2B10 to human liver microsomal cotinine N-glucuronidation were investigated using the selective inhibitors hecogenin (UGT1A4; Uchaipichat et al., 2006a) and desloratadine (Kazmi et al., 2015b and *Results*). The effects of each inhibitor (10 μM) were determined at each of four cotinine concentrations (0.25, 1, 3, 6 mM) following the procedure described in *Cotinine N-glucuronidation by recombinant UGTs and HLM*. The formation of cotinine N-glucuronide in the presence of desloratadine or hecogenin or a combination of both was compared with metabolite production in the absence of the inhibitors.

Kinetic Characterization of Amitriptyline, Doxepin, and Mianserin Inhibition of Human Liver Microsomal Cotinine N-Glucuronidation. The kinetics and mechanism of the inhibition of cotinine N-glucuronidation by amitriptyline, doxepin, and mianserin were characterized with HLM as the enzyme source following the method described above. Experiments to characterize inhibitor constants (K_i) employed HLM (0.5 mg/ml) supplemented with BSA (1% w/v). Effects of four added concentrations (1, 2.5, 5, and 10 μM) of each of amitriptyline, doxepin, and mianserin were characterized at each of the three added cotinine concentrations (1, 2, and 3 mM). Concentrations of each of the inhibitors were corrected for nonspecific binding to HLM and BSA.

Measurement of the Nonspecific Binding of Cotinine to Supersomes, HLM, and BSA, and Amitriptyline, Doxepin, and Mianserin to HLM and BSA. Nonspecific binding experiments were performed using rapid equilibrium dialysis (RED) devices fitted with an 8-kDa molecular weight cutoff cellulose membrane, as described by Pattanawongsa et al. (2015). For the assessment of cotinine binding, the sample chamber was loaded with cotinine (0.1–15 mM) and Supersome protein (1 mg/ml) or HLM (0.5 mg/ml) or BSA (1% w/v), in 0.1 M phosphate buffer (pH 7.4, total volume 100 μl). The buffer chamber was loaded with 300 μl 0.1 M phosphate buffer (pH 7.4). Experiments were also performed with buffer-buffer, enzyme-enzyme, and BSA-BSA controls. The RED devices were incubated at 37°C for 5 hours, by which time equilibrium had been achieved. A 30 μl aliquot was collected from each chamber, and protein was precipitated with 0.3 μl 11.6 M HClO$_4$, or with 0.9 μl 11.6 M HClO$_4$ for samples containing BSA. Samples were cooled on ice for 10 minutes and then centrifuged (5000g) at 4°C for 10 minutes. A 10 μl aliquot was diluted with 90 μl 5% acetonitrile in water. Cotinine was analyzed by HPLC following the procedure described for cotinine N-glucuronide, but using 83% mobile phase A and 17% mobile phase B. Under these conditions, the retention time of cotinine was 4.6 minutes.

The binding of amitriptyline, doxepin, and mianserin (2, 5, 10, and 25 μM) to HLM (0.5 mg/ml) plus BSA (1% w/v) was similarly measured using the RED device. Like cotinine, experiments were performed with buffer-buffer and protein-protein controls. After 8-hour equilibration, a 70 μl aliquot was taken from each chamber and mixed with four volumes of 4% acetic acid in methanol,

which also contained the assay internal standard (Supplemental Table 1). Samples were cooled on ice for 10 minutes, and then centrifuged (5,000g) at 4°C for 10 minutes. The supernatant fraction was decanted and evaporated to dryness using a miVac modular concentrator (Genevac, Suffolk, UK). The residue was reconstituted in 50 μL mobile phase and analyzed by HPLC (see (Supplemental Table 1 for conditions).

Molecular Modeling. The three-dimensional coordinates (sdf format) of dataset molecules were obtained from the Pubchem server (https://pubchem.ncbi.nlm.nih.gov/). The molecules were imported into SYBYL (version X-2.1, CERTARA, Princeton, NJ) and geometry optimized using the AM1 Hamiltonian (MOPAC). All molecular modeling was performed using SYBYL installed on Macintosh workstation running on OS X 10.9.5 operating system. The structural overlay of molecules was undertaken using the Surflex-Sim program (Jain, 2000, 2004), which utilizes the morphologic similarity approach to generate alignments of molecules. Similarity is defined as a Gaussian function of the differences in the molecular surface distances of two molecules at weighted observation points on a uniform grid. The computed surface represents distances to the nearest atomic surface and distances to donor and acceptor surfaces. Amitriptyline, one of the most potent UGT2B10 inhibitors (see *Results*), was used as the template for the overlay of dataset molecules. The overlay quality of the dataset molecules was evaluated by measuring the distance between key pharmacophoric features, including the centroid of either of the phenyl rings (present in the tricyclic structure of amitriptyline) and the aryl ring (closest) of the dataset molecule observed in the alignment. Moreover, the distances between the side-chain amine N atom of amitriptyline and the dataset molecules (aliphatic or alicyclic) were also estimated. The smaller the distance, the more closely the pharmacophoric features overlay between amitriptyline and the dataset molecule. In addition, for tri- and tetracyclic compounds, the angles between the rings of the tricyclic scaffold were measured by defining a centroid for each ring on the geometry optimized structures. The torsion angles were measured for the bridge (-CH$_2$-X where X= -CH$_2$, -O, or -N) connecting the two aromatic rings of the tricyclic scaffold. For example, in the case of amitriptyline, the torsion angle was measured for the dimethylene (-CH$_2$-CH$_2$-) bridge of the central seven-membered (cycloheptene) ring.

Data Analysis. The Michaelis-Menten equation (eq. 1) was fit to kinetic data for cotinine N-glucuronidation by UGT2B10 and HLM ($\pm$1% BSA) using Enzfitter (version 2.0, Biosoft, Cambridge, UK) to obtain values of K_m and V_{max}. Inhibitor constants, based on unbound concentrations of amitriptyline, doxepin, and mianserin present in incubations ($K_{i,u}$), were determined by fitting the expressions given in eq. 2–4 to experimental data using Enzfitter. Goodness of fit of all expressions was assessed from comparison of the parameter S.E. of fit, coefficient of determination (r^2), 95% confidence intervals, and F-statistic.

Equation 1, Michaelis-Menten equation:

$$v = \frac{V_{max} \times [S]}{K_m + [S]}$$

where v is the rate of product formation, V_{max} is maximal velocity, [S] is substrate concentration, and K_m is the Michaelis constant.

Equation 2, competitive inhibition:

$$v = \frac{V_{max} \times [S]}{K_m(1 + [I]/K_i) + [S]}$$

where [I] is the inhibitor concentration and K_i is the inhibitor constant (for the EI complex).

Equation 3, noncompetitive inhibition:

$$v = \frac{V_{max} \times [S]}{(1 + [I]/K_i)(K_m + [S])}$$

where K_i is the inhibitor constant for the EI and ESI complexes.

Equation 4, mixed (competitive–noncompetitive) inhibition:

$$v = \frac{V_{max} \times [S]}{K_m(1 + [I]/K_i) + [S](1 + [I]/K_i')}$$

where K_i and K_i' are the inhibitor constants for the EI and ESI complexes, respectively.

IC$_{50}$ values were determined according to equation 5:

$$v_{i=} \; v_0 \left[1 - \frac{[I]}{([I] + IC_{50})} \right]$$

where v_0 is the control activity and v_i is the activity in the presence of the inhibitor (I).

For a drug metabolized by a single enzyme along a single metabolic pathway, the extent of inhibition of the hepatic clearance by a coadministered drug [determined as the ratio of the areas under the plasma drug concentration–time curves (AUC) with and without inhibitor coadministration] may be calculated according to eq. 6, which is valid for competitive and noncompetitive inhibition:

$$\frac{AUC_i}{AUC} = \; 1 + \frac{[I]}{K_i}$$

where [I] is the inhibitor concentration. Optimally, [I] is taken as the hepatic inlet concentration (Miners et al., 2010b), but given the unavailability of key pharmacokinetic parameters (particularly absorption rate constant) for amitriptyline, doxepin, and mianserin, the maximum drug plasma concentration (C$_{max}$) was used as the estimate of [I] in the calculation of the AUC ratio. Amitriptyline (50 mg dose): mean C$_{max}$ 0.15 μM (Kukes et al., 2009), fraction unbound in plasma (fu) 0.065 (Baumann et al., 1986). Assuming linear kinetics, the C$_{max}$ expected for a single 150 mg dose of amitriptyline is 0.45 μM. Doxepin (50 mg dose): mean C$_{max}$ 0.29 μM (Virtanen et al., 1980), fu 0.79 (Faulkner et al., 1983). Again, assuming linear kinetics, the C$_{max}$ expected for a single 150 mg dose of doxepin is 0.87 μM. Mianserin (60 mg dose): mean C$_{max}$ 0.38 μM (Hrdina et al., 1983), fu 0.055 (Kristensen et al., 1985).

Statistical comparisons of kinetic constants reported in Table 1 were performed using the Mann-Whitney U test with SPSS version 22 (SPSS, Chicago, IL). P values <0.05 were considered significant.

Results

Kinetics of Cotinine N-Glucuronidation. Cotinine N-glucuronidation by recombinant UGT2B10 and HLM ($\pm$BSA, 1% w/v) followed Michaelis-Menten kinetics (Fig. 1). Mean ($\pm$S.D.) kinetic constants are given in Table 1. The mean K$_m$ for human liver microsomal cotinine N-glucuronidation was marginally higher ($P = 0.06$) than that for UGT2B10, whereas the V$_{max}$ with HLM as the enzyme source was 6.8-fold higher compared with UGT2B10. The activities of numerous UGTs, particularly with HLM as the enzyme source, are known to be increased in the presence of BSA (0.5–2% w/v) due to sequestration of inhibitory membrane long-chain unsaturated fatty acids released during the course of an incubation (Rowland et al., 2007, 2008; Kilford et al., 2009; Manevski et al., 2011; Walsky et al., 2012). Addition of BSA (1% w/v) to incubations of HLM resulted in a 45% reduction in K$_m$ and a small (11%) but statistically significant increase in V$_{max}$. The mean Cl$_{int}$, calculated as V$_{max}$/K$_m$, for human liver microsomal cotinine N-glucuronidation derived in the presence of BSA was approximately double that determined in the absence of BSA. Cotinine was shown not to bind (fu$_{,mic}$ > 0.95) to Supersomes (1 mg.ml), HLM (0.5 mg/ml), or

BSA (1% w/v). Thus, correction of K$_m$ and Cl$_{int}$ values for substrate-binding HLM and BSA was not required.

Confirmation of the UGT2B10 Substrate Selectivity of Cotinine and Inhibitor Selectivity of Desloratadine and Nicotine. Cotinine N-glucuronidation by UGT 1A1, 1A3, 1A4, 1A6, 1A7, 1A8, 1A9,
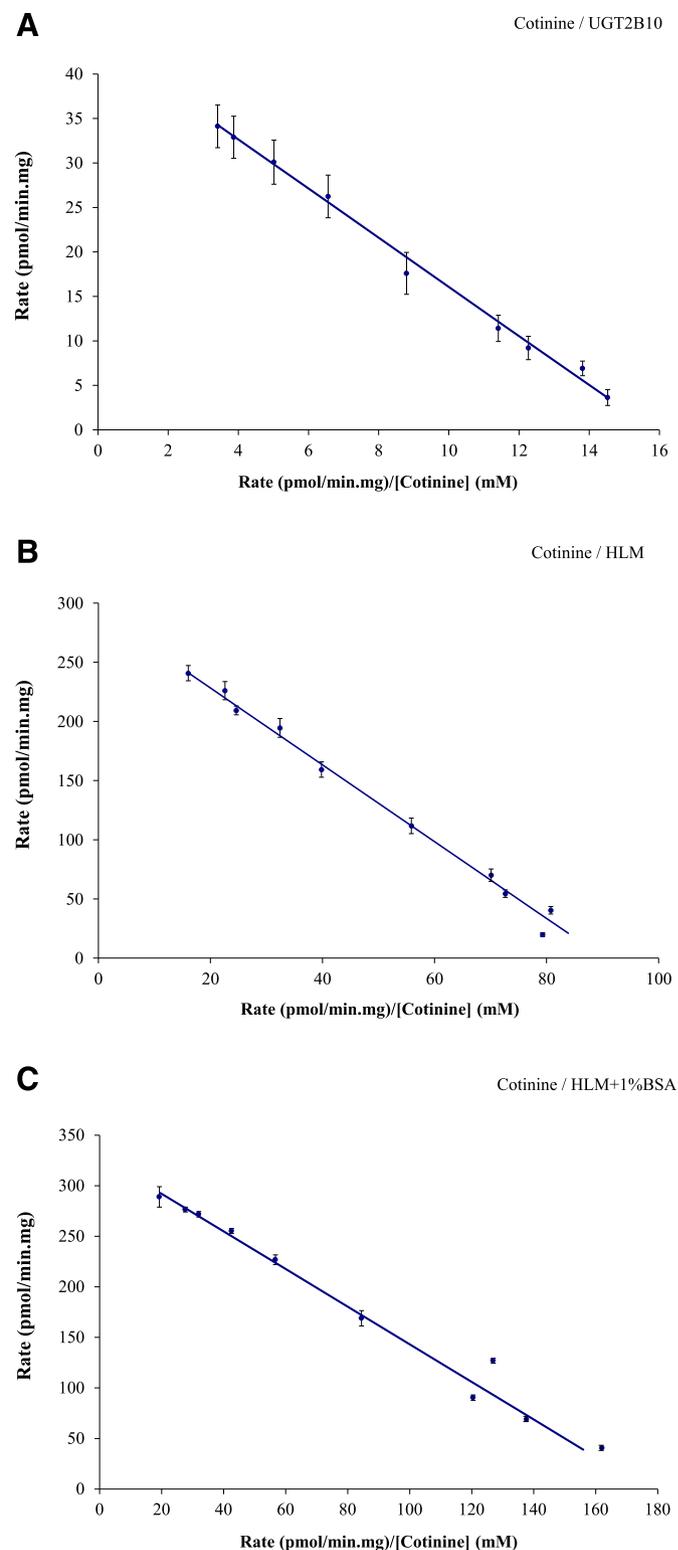
Fig. 1. Eadie-Hofstee plots for cotinine N-glucuronidation by recombinant UGT2B10 (A), HLM (B), and HLM plus BSA (C). Points with error bars represent the mean $\pm$ S.D. of four to six replicates.

TABLE 1

Derived kinetic constants for cotinine N-glucuronidation by recombinant UGT2B10 and human liver microsomes ($\pm$BSA, 1% w/v)

Kinetic Parameter	Enzyme Source		
	Recombinant UGT2B10	HLM	HLM + BSA
K$_m$ (mM)	2.78 ± 0.34	3.34 ± 0.39	1.85 ± 0.07[b]
V$_{max}$ (pmol/min.mg)	43.7 ± 2.29	297 ± 14.5[a]	329 ± 4.56[b]
CL$_{int}$ (μl/min.mg)	15.9 ± 2.48	89.7 ± 7.99[a]	178 ± 4.41[b]

Kinetic parameters expressed as mean $\pm$ S.D. of four to six replicates.
[a] $P < 0.05$ compared with recombinant UGT2B10.
[b] $P < 0.05$ compared with HLM without BSA.

1A10, 2B4, 2B7, 2B10, 2B15, and 2B17 was investigated at three substrate concentrations (0.25, 1, and 5 mM) that spanned the K_m values reported in Table 1. Activity was observed only with UGT1A4 and UGT2B10. The respective mean N-glucuronidation rates by

UGT2B10 at the three cotinine concentrations were 6.0, 15.4, and 38.0 pmol/min.mg. By contrast, with UGT1A4 as the enzyme source, cotinine N-glucuronidation (2.3 pmol/min.mg) was observed at just the highest substrate concentration.
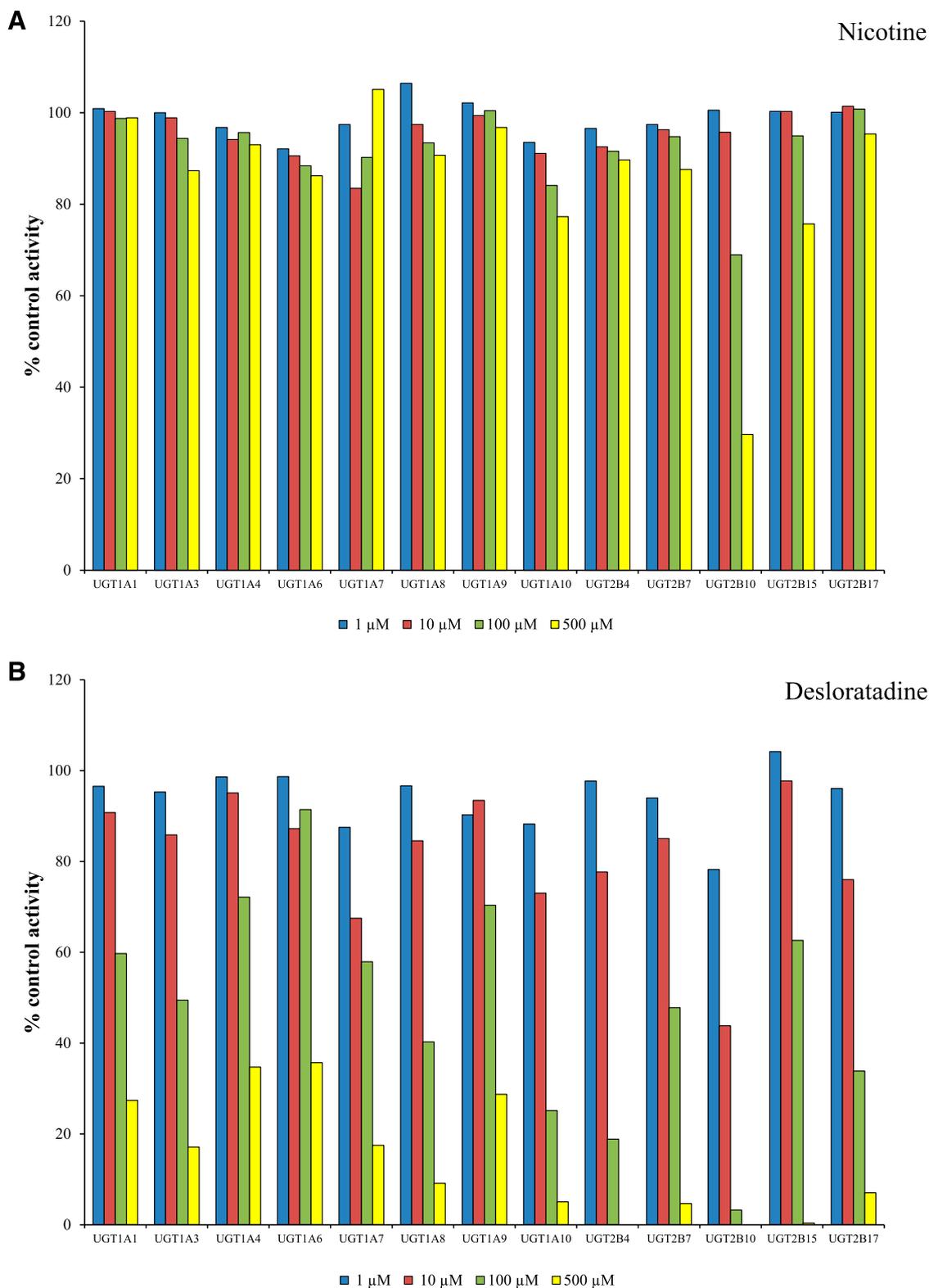
Fig. 2. Inhibition of recombinant human UGT enzymes by nicotine (A) and desloratadine (B). Each bar represents the mean of duplicate measurements (<5% variance). See *Materials and Methods* for experimental conditions.

Nicotine and desloratadine (1, 10, 100, and 500 μM) were screened for inhibition of UGT 1A1, 1A3, 1A4, 1A6, 1A7, 1A8, 1A9, 1A10, 2B4, 2B7, 2B10, 2B15, and 2B17. Over the concentration range investigated, nicotine inhibited only UGT2B10 with an IC_{50} < 500 μM (Fig. 2A); the mean ($\pm$S.E. of parameter fit) IC_{50} value was 214 $\pm$ 2.9 μM. Consistent with the recent report of Kazmi et al. (2015b), desloratadine potently inhibited UGT2B10 (IC_{50} 3.86 $\pm$ 0.05 μM). IC_{50} values for other hepatically expressed UGT enzymes ranged from 18.9 $\pm$ 0.10 μM for UGT2B4 to 271 $\pm$ 7.6 μM for UGT1A6 (Fig. 2B; (Supplemental Table 2). In general, the inhibition observed in this study for desloratadine (10 μM) is in good agreement to that reported by Kazmi et al. (2015b) for hepatically expressed UGT enzymes, except UGT2B4, which was not investigated by these authors.

Inhibition of Recombinant UGT2B10 by UGT Enzyme-Selective Inhibitors. Effects of putative UGT enzyme-selective inhibitors on recombinant UGT2B10 activity were assessed using cotinine as the substrate probe. The UGT1A4 inhibitor hecogenin (1–100 μM) was without effect on UGT2B10 activity (Table 2), consistent with the observations of Guo et al. (2011) and Kato et al. (2013). Niflumic acid, which inhibits UGT1A9 with a K_i of 0.10 μM and UGT1A1 and UGT2B15 with respective K_i values of 18 and 62 μM (Miners et al., 2011), inhibited UGT2B10 with an IC_{50} of 168 $\pm$ 0.14 μM (Table 2). Fluconazole, employed as a selective inhibitor of UGT2B4 and UGT2B7 (Uchaipichat et al., 2006b; Raungrut et al., 2010), inhibited UGT2B10 with an IC_{50} of 1136 $\pm$ 88.4 μM (Table 2), whereas phenylbutazone, which has been reported to be a relatively selective inhibitor of UGT1A subfamily enzyme activities (Uchaipichat et al., 2006a), inhibited UGT2B10 with an IC_{50} of 220 $\pm$ 35.4 μM. The effect of fluconazole on UGT2B10 prompted us to investigate the effects of two other azole antifungal agents, itraconazole and ketoconazole. Whereas itraconazole was without effect on UGT2B10, ketoconazole was a relatively potent inhibitor of this enzyme (IC_{50} = 11.9 $\pm$ 1.7 μM; Table 2).

The Contribution of UGT2B10 to Human Liver Microsomal Cotinine N-Glucuronidation. As shown above, of the hepatically expressed enzymes in the UGT 1A and 2B subfamilies, only UGT1A4 and UGT2B10 glucuronidated cotinine. Inhibition studies with hecogenin and desloratadine were performed to elucidate the relative contributions of these enzymes to human liver microsomal cotinine N-glucuronidation. Effects of desloratadine and hecogenin (both 10 μM), separately and combined, were determined at four cotinine concentrations that spanned the K_m for cotinine N-glucuronidation by HLM (viz. 0.25, 1, 3, and 6 mM). Hecogenin had a negligible effect (<10% inhibition) at all cotinine concentrations (Fig. 3). By contrast, desloratadine, alone and in combination with hecogenin, inhibited human liver microsomal cotinine N-glucuronidation to a near-identical extent (Fig. 3). It should be noted that the extent of cotinine N-glucuronidation observed with 10 μM desloratadine is broadly consistent with IC_{50} for desloratadine (~4 μM) reported in Table 2. Consistent with competitive inhibition by desloratadine (Kazmi et al., 2015b), greater and lesser inhibition occurred at cotinine concentrations below and above the K_m, respectively. Collectively, the data indicate that cotinine is a selective substrate of human liver microsomal UGT2B10.

Inhibition of Recombinant UGT2B10 by Antidepressant and Antipsychotic Drugs: Modeling and Structure-Activity Relationships. Thirty-four antidepressant drugs (including didesmethylimipramine and desmethylnortriptyline, the respective demethylated metabolites of desipramine and nortriptyline) were screened as potential inhibitors of UGT2B10 (Table 2). The most potent inhibition was observed for mianserin, doxepin, and amitriptyline, which have IC_{50} values in the range 2.2–6.5 μM. IC_{50} values for the structurally related compounds loratadine and desloratadine were also in this range (Table 2). Twenty-five compounds additionally exhibited moderately potent inhibition

TABLE 2

IC_{50} values for the inhibition of recombinant UGT2B10 by UGT enzyme-selective inhibitors, azoles, and antidepressant and antipsychotic drugs

| Classification	Drug	IC_{50} (μM) $\pm$ S.E. of Parameter Fit[a]
UGT enzyme-selective inhibitors		
	Desloratadine	3.86 $\pm$ 0.05
	Fluconazole	1136 $\pm$ 88.4
	Hecogenin	NI
	(-)-Nicotine	214 $\pm$ 2.86
	Niflumic acid	168 $\pm$ 0.14
	Phenylbutazone	220 $\pm$ 35.4
	Loratadine (desloratadine precursor)	2.18 $\pm$ 0.34
Azoles		
	Itraconazole	NI
	Ketoconazole	11.9 $\pm$ 1.69
Antidepressants		
TCAs		
Primary amine[b]	Desmethylnortriptyline	43.7 $\pm$ 2.03
	Didesmethylimipramine	36.2 $\pm$ 0.40
Secondary amine	Desipramine	34.1 $\pm$ 1.04
	Norclomipramine	50.8 $\pm$ 4.88
	Nortriptyline	45.3 $\pm$ 0.02
	Protriptyline	34.3 $\pm$ 0.40
Tertiary amine	Amitriptyline	6.45 $\pm$ 0.46
	Clomipramine	26.0 $\pm$ 0.49
	Doxepin	3.64 $\pm$ 0.16
	Imipramine	42.8 $\pm$ 1.52
	Trimipramine	32.6 $\pm$ 1.70
Tetracyclic antidepressants		
Tertiary amine	Mianserin	2.24 $\pm$ 0.11
	Mirtazapine	31.0 $\pm$ 0.99
SSRIs		
Primary amine	Fluvoxamine	224 $\pm$ 6.11
Secondary amine	Fluoxetine	72.4 $\pm$ 15.8
	Paroxetine	63.5 $\pm$ 4.79
	Sertraline	92.7 $\pm$ 8.99
Tertiary amine	Citalopram	218 $\pm$ 17.4
SNRIs		
Secondary amine	Duloxetine	81.2 $\pm$ 8.17
Tertiary amine	Desvenlafaxine	440 $\pm$ 16.5
	Venlafaxine	NI
MAOIs		
Primary amine	Tranylcypromine	NI
Tertiary amine	Selegiline	67.2 $\pm$ 3.60
Hydrazine	Phenelzine	94.2 $\pm$ 1.79
Antipsychotics		
Typical antipsychotics		
Tertiary amine	Chlorpromazine	79.0 $\pm$ 10.7
	Fluphenazine	53.5 $\pm$ 6.54
	Haloperidol	NI
	Loxapine	36.0 $\pm$ 1.82
	Perphenazine	66.2 $\pm$ 0.6
	Thioridazine	71.3 $\pm$ 18.2
Atypical antipsychotics		
Tertiary amine	Aripiprazole	55.8 $\pm$ 0.80
	Clozapine	61.3 $\pm$ 1.40
	Olanzapine	276 $\pm$ 4.49
	Quetiapine	43.9 $\pm$ 7.65

NI, negligible inhibition over the concentration range investigated.

[a]IC_{50} values were calculated by fitting eq. 5 to experimental data using Enzfitter (see *Materials and Methods*). Each IC_{50} value was derived from duplicate measurements at each of four inhibitor concentrations with cotinine as the substrate (see *Materials and Methods*). S.E. is the standard error of the parameter fit from Enzfitter.

[b]The designation of primary, secondary, or tertiary amine or hydrazine refers to the N-containing functional group present in the side chain (aliphatic or alicyclic) attached to the mono-, bi-, tri-, or tetracyclic structure (Supplemental Fig. 1).

(IC_{50} values 26–94 μM), whereas six were weak (IC_{50} > 200 μM) or noninhibitors.

Ligand-based approaches were employed to identify the structural features associated with significant inhibition. The majority of significant inhibitors (arbitrarily defined as having an IC_{50} < 100 μM) are generally tri- or tetracyclic structures with an amine-containing side chain (aliphatic
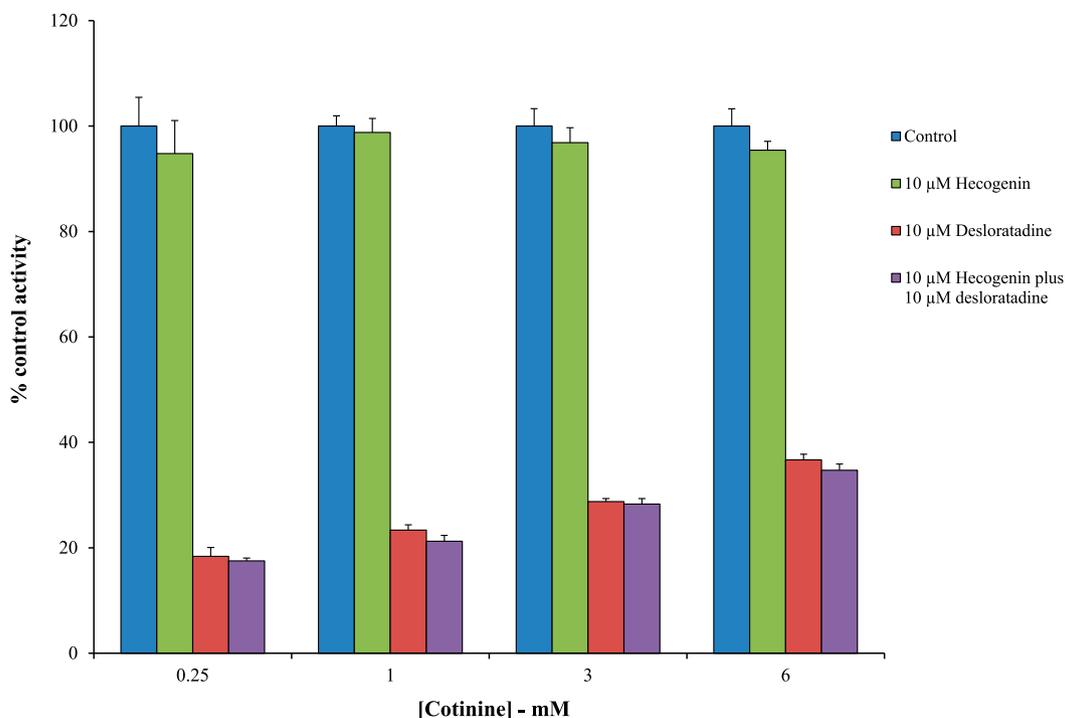
Fig. 3. Inhibition of human liver microsomal cotinine N-glucuronidation at four substrate concentrations (0.25, 1, 3, and 6 mM) by hecogenin (10 μM), desloratadine (10 μM), and hecogenin plus desloratadine. Each bar represents the mean $\pm$ S.D. of quadruplicate measurements.

or alicyclic), although exceptions occur. All of the tricylic and tetracyclic compounds, except olanzapine, overlaid well on the structure of amitriptyline (Fig. 4). Olanzapine is the only compound investigated in this work with a five-membered ring in the tricyclic scaffold, which results in a different geometry and poor overlay (Supplemental Fig. 2). The bis-ring structure of fluoxetine permits adoption of a conformation similar to that of amitriptyline, resulting in a reasonable overlay. Of the bicyclic compounds that exhibited significant inhibition, aripiprazole, duloxetine, and paroxetine aligned reasonably well with the structure of amitriptyline (Supplemental Fig. 2), whereas partial overlay was observed for sertraline (IC$_{50}$ 92.7 μM), presumably due to the shorter distance between the ring scaffold and side-chain amine group. Poor overlay of the SSRIs citalopram and fluvoxamine, including the side-chain amine of the latter (which aligns 3.3 Å from the side chain N of amitriptyline), provides an explanation for the weak inhibition observed with these compounds. Overlay on the structure of amitriptyline for the remaining compounds screened for inhibition (viz. haloperidol, venlafaxine, desvenlafaxine, and the MAOIs phenelzine, selegiline, and tranylcypromine), all of which lack a fused ring scaffold, was generally consistent with the observed potency of UGT2B10 inhibition (Supplemental Fig. 2).

Compared with other TCAs, the potent UGT2B10 inhibitors amitriptyline and doxepin share in common a side-chain tertiary amine functional group linked to the central cycloheptene ring by a double bond rather than to a potentially invertible N atom (Supplemental Fig. 1). The exocyclic double bond present in loratadine and desloratadine and the fused piperidine ring present in mianserin similarly confer structural rigidity. Near-identical geometries were observed for amitriptyline, doxepin, desloratadine, and loratadine, and, consequently, there was near-complete overlap of structural features (Fig. 5A). By contrast, conformational differences occur around the CH$_2$-X moiety of the cycloheptene ring of other TCAs (e.g., imipramine), and the ring scaffold of tricyclic compounds with a six-membered central ring (e.g., chlorpromazine) is more planar (Fig. 5, B and C).

The Kinetics of Amitriptyline, Doxepin, and Mianserin Inhibition of Human Liver Microsomal UGT2B10 and In Vitro–In Vivo Extrapolation. Given the potent inhibition of UGT2B10 observed for amitriptyline, doxepin, and mianserin, kinetic studies were performed to determine the K_i values for inhibition of human liver microsomal cotinine N-glucuronidation. Incubations were supplemented with 1% w/v BSA (see above). Concentrations of amitriptyline,
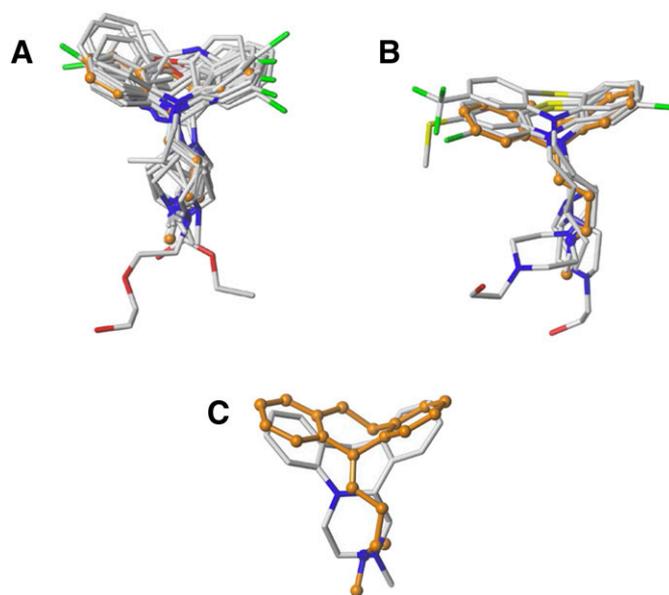
Fig. 4. Overlay of tri- and tetracyclic dataset molecules on the structure of amitriptyline. C atoms of amitriptyline and overlaid molecules are shown in orange and white, respectively, whereas O, N, S, and Cl atoms are shown in red, blue, yellow, and green, respectively. (A) Overlay of tricyclic molecules with a central seven-membered ring scaffold. (B) Overlay of tricyclic molecules with central six-membered ring scaffold. (C) Overlay of the tetracyclic molecule mianserin.
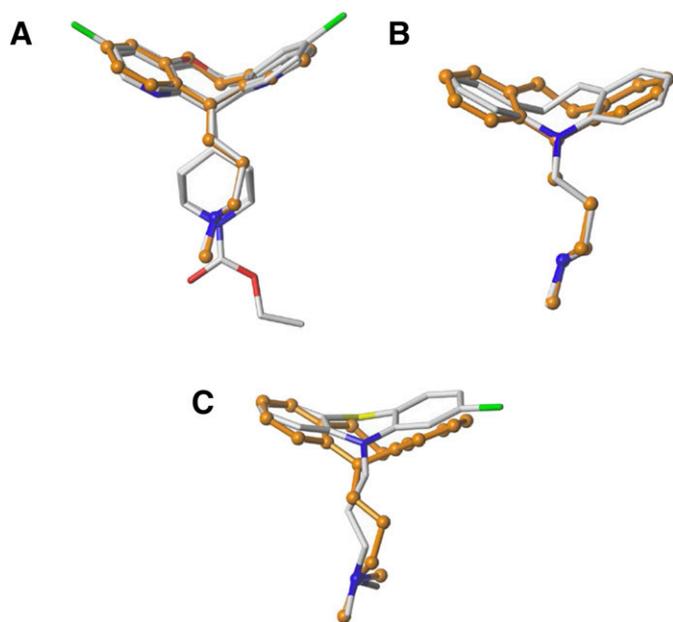
Fig. 5. Overlay of representative molecules with a tricyclic scaffold on the structure of amitriptyline. C atoms of amitriptyline and overlaid molecules are shown in orange and white, respectively, whereas O, N, S, and Cl atoms are shown in red, blue, yellow, and green, respectively. (A) Overlay of doxepin, desloratadine, and loratadine. (B) Overlay of imipramine. (C) Overlay of chlorpromazine.

doxepin, and mianserin were corrected for binding to HLM and BSA, and the inhibitor constants therefore represent $K_{i,u}$ values. The binding of each compound was independent of added concentration across the range 2–25 μM. Mean ($\pm$S.D.) values of fu_{mic} for amitriptyline, doxepin, and mianserin were 0.32 $\pm$ 0.03, 0.42 $\pm$ 0.03, and 0.20 $\pm$ 0.01, respectively. As noted above, cotinine does not bind to either HLM or BSA. Amitriptyline, doxepin, and mianserin competitively inhibited human liver microsomal cotinine N-glucuronidation with mean $K_{i,u}$ ($\pm$S.D.) values of 0.61 $\pm$ 0.05, 0.95 $\pm$ 0.18, and 0.43 $\pm$ 0.01 μM (Fig. 6).

Using the plasma concentrations for amitriptyline, doxepin, and mianserin given above (for doses at the upper end of the usual recommended dosage ranges; viz. 150, 150, and 60 mg/d, respectively), respective $[I]/K_{i,u}$ ratios based on total drug concentration are 0.74, 0.92, and 0.88; corresponding values of $1 + [I]/K_{i,u}$ (see eq. 6 above) for amitriptyline, doxepin, and mianserin are 1.74, 1.92, and 1.88, respectively. When $[I]$ is taken as the unbound concentration of drug in plasma (i.e., the product of drug plasma concentration and fu), $[I]/K_{i,u}$ values are <0.2.

Discussion

Initial studies confirmed that cotinine is a selective substrate for UGT2B10, and desloratadine and nicotine are relatively selective inhibitors of this enzyme. Cotinine N-glucuronidation by HLM followed Michaelis-Menten kinetics, consistent with the predominant involvement of a single UGT enzyme in this reaction. It has been reported previously that only UGT 1A4 and 2B10 glucuronidate cotinine (Kuehl and Murphy, 2003; Kaivosaari et al., 2007). This was confirmed in this work, although the cotinine N-glucuronidation activity of UGT1A4 was very low. To further elucidate the relative contributions of UGT2B10 and UGT1A4 to human liver microsomal cotinine N-glucuronidation, inhibition experiments were conducted with desloratadine and the UGT1A4 selective inhibitor hecogenin (Uchaipichat et al., 2006a). The separate and combined effects of
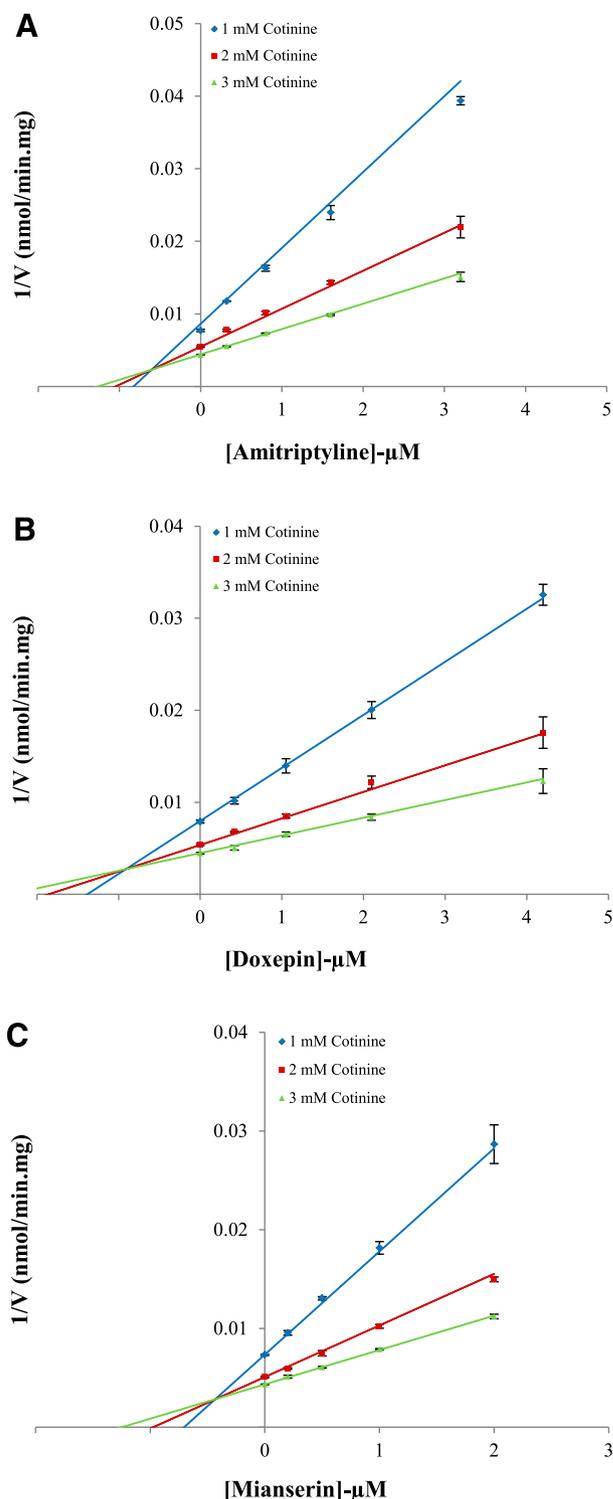
Fig. 6. Dixon plots for the inhibition of human liver microsomal cotinine N-glucuronidation by amitriptyline (A), doxepin (B), and mianserin (C). Incubations contained BSA (1% w/v). Points represent the mean $\pm$ S.D. of quadruplicate measurements. Inhibitor concentrations are corrected for binding to HLM plus BSA. See *Materials and Methods* for experimental conditions.

desloratadine and hecogenin shown in Fig. 3 demonstrate that UGT2B10 is responsible for >90% of cotinine N-glucuronidation by HLM, making this compound a convenient, readily available UGT2B10 substrate probe. Moreover, compared with many other UGT enzyme-selective substrate probes, cotinine does not bind to BSA

(or HLM) and hence correction for nonspecific and protein binding is not required.

Consistent with the recent report of Kazmi et al. (2015b), desloratadine was shown to be a moderately selective inhibitor of UGT2B10 (Fig. 2B). The IC$_{50}$ for UGT2B10 inhibition is approximately an order of magnitude lower than that for UGT2B4, the next most potently inhibited enzyme. UGT2B4 was not screened for inhibition in the study of Kazmi et al. (2015b). Thus, it may not be possible to differentiate relative contributions of UGT2B10 and UGT2B4 when desloratadine (10 μM; Kazmi et al., 2015b) is used for reaction phenotyping. Previous studies have reported that nicotine inhibits UGT2B10, but not UGT1A4 (Zhou et al., 2010). Similar specificity was observed in this study, although nicotine was observed to additionally inhibit UGT2B15, albeit less potently than UGT2B10.

Previously reported K$_m$ and V$_{max}$ values for cotinine N-glucuronidation by HLM range from 0.93 to 5.43 mM and 643 to 696 pmol/min.mg, respectively (Ghosheh and Hawes, 2002; Nakajima et al., 2002; Chen et al., 2007; Kaivosaari et al., 2007), whereas K$_m$ values of 0.47 and 1.0 mM have been reported for cotinine N-glucuronidation by recombinant UGT2B10 (Chen et al., 2007; Kaivosaari et al., 2007). The mean K$_m$ (2.78 mM) and V$_{max}$ (297 pmol/mg.min) values for human liver microsomal cotinine N-glucuronidation determined in this study tended to be higher and lower, respectively, than previously reported values. The reasons for this are unclear, although 89-fold variability in the rates of nicotine N-glucuronidation has been observed in a panel of microsomes from 14 livers (Nakajima and Yokoi, 2005). The commercially sourced HLM employed in this study were a pool from 150 donors (equal numbers of males and females), whereas most reports have generally used microsomes from fewer donors (Ghosheh and Hawes, 2002; Nakajima et al., 2002; Kaivosaari et al., 2007). Similarly, previous studies with UGT2B10 have used different expression systems to the Supersomes used in this work. Nevertheless, the differences in reported K$_m$ values are surprising. Of note, we have found that the UGT2B10 activity of Supersomes remains stable for at least 6 months.

The addition of BSA (0.5–2% w/v) to incubations has been reported to decrease the K$_m$ values (with occasional effects on V$_{max}$) for substrates of several hepatically expressed UGT enzymes, particularly UGT 1A9, 2B4, 2B7, and 2B15 (Rowland et al., 2007, 2008; Kilford et al., 2009; Manevski et al., 2011, 2013; Walsky et al., 2012). The albumin effect appears to arise from sequestration of inhibitory membrane fatty acids released during the course of an incubation. The effect of lower concentrations of BSA has been reported to be substrate dependent (Manevski et al., 2013), but this may arise from incomplete sequestration of inhibitory fatty acids at BSA concentrations <0.5% w/v. Addition of BSA (1% wv) was found in this work to reduce the K$_m$ for human liver microsomal nicotine N-glucuronidation by approximately 50%, with a small (11%) but statistically significant increase in V$_{max}$. Thus, subsequent inhibition kinetic studies included BSA to determine K$_i$ values accurately. Furthermore, HLM were preferred to UGT2B10 in these studies due to the considerably lower cost of HLM compared with the recombinant enzyme.

UGT enzyme-selective inhibitors are a valuable experimental tool for the reaction phenotyping of human liver microsomal drug and chemical glucuronidation (Miners et al., 2010a). However, previous studies that have characterized UGT enzyme inhibition selectivity have generally excluded UGT2B10. Niflumic acid at a concentration of 2.5 μM is considered a highly selective inhibitor of UGT1A9 (Miners et al., 2011), whereas at 100 μM it additionally inhibits UGT1A1 and UGT2B15. The IC$_{50}$ for niflumic acid inhibition of UGT2B10 observed in this study (168 μM) confirms the UGT1A9 inhibition selectivity of niflumic acid at a low concentration, but indicates that this compound

will significantly inhibit UGT2B10 as well as UGT1A1 and UGT2B15 at a concentration of 100 μM. As noted above, hecogenin does not inhibit UGT2B10, consistent with the reported inhibition selectivity for UGT1A4 (Uchaipichat et al., 2006b). By contrast, fluconazole (2.5 mM), which is considered a selective inhibitor of UGT2B4 and UGT2B7, inhibited UGT2B10 to a similar extent to that reported for UGT2B4/7 (Uchaipichat et al., 2006a; Raungrut et al., 2010). The latter observation prompted us to investigate UGT2B10 inhibition by two additional azole antifungals: itraconazole and ketoconazole. Although the triazole itraconazole was without effect on UGT2B10, the imidazole ketoconazole was a relatively potent inhibitor of this enzyme (IC$_{50}$ = 11.9 ± 1.7 μM). Similar to the inhibition selectivity of fluconazole, ketoconazole has previously been reported to be a relatively potent inhibitor of UGT2B4 (Raungrut et al., 2010) and an inhibitor of UGT2B7 (Takeda et al., 2006).

Previous studies have shown that the TCAs amitriptyline, clomipramine, imipramine, and trimipramine and the atypical antipsychotic olanzapine are substrates and/or inhibitors of UGT2B10 (Chen et al., 2007; Zhou et al., 2010; Guo et al., 2011; Kato et al., 2013). As noted in the *Introduction*, antidepressant and antipsychotic drugs typically contain an amine functional group. Thus, nine TCAs (plus the respective N-demethylated metabolites of desipramine and nortriptyline), five SSRIs, three SNRIs, three MAOIs, the tetracyclic antidepressants mianserin and mirtazapine, and six typical and four atypical antipsychotic drugs were screened for inhibition of UGT2B10. Although the majority of the compounds investigated inhibited UGT2B10 with IC$_{50}$ values <100 μM, most potent inhibition was observed for the TCAs amitriptyline and doxepin and the tetracyclic mianserin. Desloratadine and loratadine were also potent inhibitors of UGT2B10. Structural interrogation of these data suggests that potent and moderate inhibition of UGT2B10 requires a hydrophobic domain (tetra-/tri-/bicyclic scaffold or an aromatic ring) and an amine (or hydrazine) functional group, which is most commonly located three bond lengths (C-C and/or C-N) from the hydrophobic domain. All but one of the potent inhibitors identified in this study, namely desloratadine, are tertiary amines. However, the presence of a tertiary amine is not an obligatory requirement for inhibition; moderate inhibition occurred with primary and secondary amines. Because the amines will be largely charged at physiologic pH, the data suggest that hydrophobic and charge interactions (e.g., with aspartic or glutamic acid) are involved in inhibitor binding.

The data also suggest that spatial features influence the potency of UGT2B10 inhibition. TCAs with a dihydrodibenzazepine moiety (e.g., clomipramine, desipramine, and imipramine) are inherently more flexible with more degrees of conformational freedom than dibenzocycloheptenes, such as amitriptyline and doxepin. It has been proposed that such conformational differences, particularly in the tricyclic ring scaffold, may be associated with differences in the receptor-binding selectivity and affinity of TCAs (Munro et al., 1987; Casarotto and Craik, 2001). As noted above and shown in Fig. 5, the relatively subtle conformational differences noted among amitriptyline, doxepin, desloratadine, and loratadine compared with other TCAs (e.g., imipramine) and tricyclic compounds with a six-membered central ring (e.g., antipsychotics such as chlorpromazine) may similarly account for differences in binding affinity to UGT2B10.

Given the potent inhibition (K$_{i,u}$ < 1 μM) of human liver microsomal UGT2B10 by amitriptyline, doxepin, and mianserin, the potential of these drugs to inhibit UGT2B10-catalyzed drug glucuronidation was explored. Estimates of 1 + [I]/K$_{i,u}$ based on total drug concentration ranged from 1.74 to 1.92 for inhibitor doses at the upper end of the usual therapeutic dosage ranges, although doses double these may be used if required (Australian Medicines Handbook, 2015). However, no

clinically significant interactions were predicted when [I] was taken as the unbound drug concentration in plasma. As we have reported previously (Rowland et al., 2006; Raungrut et al., 2010; Pattanawongsa et al., 2015), prediction of DDI potential from in vitro data for drugs cleared by glucuronidation appears to be more accurate when [I] is taken as total drug concentration, despite the fact that unbound concentration in blood is expected to reflect the hepatocellular concentration. Based on the reported K_i for desloratadine ($\sim$1 μM), Kazmi et al. (2015b) predicted a 2.2-fold increase in the AUC ratio for UGT2B10 substrates, which is similar to that proposed in this work for amitriptyline, doxepin, and mianserin. It is noteworthy that few compounds appear to be solely metabolized by UGT2B10, although the clearance of the experimental antipsychotic agent RO5263397 appears to be mediated largely by UGT2B10 (Fowler et al., 2015).

The potent inhibition of UGT2B10 by several drugs observed in this study is consistent with previous reports from this laboratory, demonstrating that inhibition of other UGT enzymes (e.g., UGT 1A1, 1A9, 2B4, and 2B7) may potentially precipitate DDIs and drug-endobiotic interactions (Boyd et al., 2006; Uchaipichat et al., 2006b; Miners et al., 2010b; Raungrut et al., 2010; Pattanawongsa et al., 2015). These observations reinforce the recent recommendations of Regulatory Agencies that new drugs should be evaluated for their potential to inhibit UGT enzymes.

Authorship Contributions

Participated in research design: Miners, Pattanawongsa, Nair, Rowland.

Conducted experiments: Pattanawongsa, Nair.

Performed data analysis: Pattanawongsa, Miners, Nair.

Wrote or contributed to the writing of the manuscript: Pattanawongsa, Miners, Nair.

References

Australian Medicines Handbook (2015) Psychotropic drugs, in *Australian Medicines Handbook* pp 767–821, Australian Medicines Handbook Pty Ltd, Adelaide, Australia.

Baumann P, Jonzier-Perey M, Koeb L, Lê PK, Tinguely D, and Schöpf J (1986) Amitriptyline pharmacokinetics and clinical response: I. Free and total plasma amitriptyline and nortriptyline. *Int Clin Psychopharmacol* 1:89–101.

Boase S and Miners JO (2002) In vitro-in vivo correlations for drugs eliminated by glucuronidation: investigations with the model substrate zidovudine. *Br J Clin Pharmacol* 54:493–503.

Boyd MA, Srasuebkul P, Ruxrungtham K, Mackenzie PI, Uchaipichat V, Stek M, Jr, Lange JMA, Phanuphak P, Cooper DA, and Udomuksorn W, et al. (2006) Relationship between hyperbilirubinaemia and UDP-glucuronosyltransferase 1A1 (UGT1A1) polymorphism in adult HIV-infected Thai patients treated with indinavir. *Pharmacogenet Genomics* 16:321–329.

Casarotto MG and Craik DJ (2001) Ring flexibility within tricyclic antidepressant drugs. *J Pharm Sci* 90:713–721.

Chen G, Blevins-Primeau AS, Dellinger RW, Muscat JE, and Lazarus P (2007) Glucuronidation of nicotine and cotinine by UGT2B10: loss of function by the UGT2B10 Codon 67 (Asp>Tyr) polymorphism. *Cancer Res* 67:9024–9029.

Chen G, Dellinger RW, Sun D, Spratt TE, and Lazarus P (2008) Glucuronidation of tobacco-specific nitrosamines by UGT2B10. *Drug Metab Dispos* 36:824–830.

Erickson-Ridout KK, Zhu J, and Lazarus P (2011) Olanzapine metabolism and the significance of UGT1A448V and UGT2B1067Y variants. *Pharmacogenet Genomics* 21:539–551.

Faulkner RD, Pitts WM, Lee CS, Lewis WA, and Fann WE (1983) Multiple-dose doxepin kinetics in depressed patients. *Clin Pharmacol Ther* 34:509–515.

Fowler S, Kletzl H, Finel M, Manevski N, Schmid P, Tuerck D, Norcross RD, Hoener MC, Spleiss O, and Iglesias VA (2015) A UGT2B10 splicing polymorphism common in African populations may greatly increase drug exposure. *J Pharmacol Exp Ther* 352:358–367.

Ghosheh O and Hawes EM (2002) N-glucuronidation of nicotine and cotinine in human: formation of cotinine glucuronide in liver microsomes and lack of catalysis by 10 examined UDP-glucuronosyltransferases. *Drug Metab Dispos* 30:991–996.

Guo J, Zhou D, and Grimm SW (2011) Liquid chromatography-tandem mass spectrometry method for measurement of nicotine N-glucuronide: a marker for human UGT2B10 inhibition. *J Pharm Biomed Anal* 55:964–971.

Hrdina PD, Lapierre YD, McIntosh B, and Oyewumi LK (1983) Mianserin kinetics in depressed patients. *Clin Pharmacol Ther* 33:757–762.

Jain AN (2000) Morphological similarity: a 3D molecular similarity method correlated with protein-ligand recognition. *J Comput Aided Mol Des* 14:199–213.

Jain AN (2004) Ligand-based structural hypotheses for virtual screening. *J Med Chem* 47:947–961.

Jin C-J, Miners JO, Lillywhite KJ, and Mackenzie PI (1993) cDNA cloning and expression of two new members of the human liver UDP-glucuronosyltransferase 2B subfamily. *Biochem Biophys Res Commun* 194:496–503.

Kaivosaari S, Toivonen P, Hesse LM, Koskinen M, Court MH, and Finel M (2007) Nicotine glucuronidation and the human UDP-glucuronosyltransferase UGT2B10. *Mol Pharmacol* 72:761–768.

Kaivosaari S, Toivonen P, Aitio O, Sipilä J, Koskinen M, Salonen JS, and Finel M (2008) Regio- and stereospecific N-glucuronidation of medetomidine: the differences between UDP-glucuronosyltransferase (UGT) 1A4 and UGT2B10 account for the complex kinetics of human liver microsomes. *Drug Metab Dispos* 36:1529–1537.

Kaivosaari S, Finel M, and Koskinen M (2011) N-glucuronidation of drugs and other xenobiotics by human and animal UDP-glucuronosyltransferases. *Xenobiotica* 41:652–669.

Kato Y, Izukawa T, Oda S, Fukami T, Finel M, Yokoi T, and Nakajima M (2013) Human UDP-glucuronosyltransferase (UGT) 2B10 in drug N-glucuronidation: substrate screening and comparison with UGT1A3 and UGT1A4. *Drug Metab Dispos* 41:1389–1397.

Kazmi F, Barbara JE, Yerino P, and Parkinson A (2015a) A long-standing mystery solved: the formation of 3-hydroxydesloratadine is catalyzed by CYP2C8 but prior glucuronidation of desloratadine by UDP-glucuronosyltransferase 2B10 is an obligatory requirement. *Drug Metab Dispos* 43:523–533.

Kazmi F, Yerino P, Barbara JE, and Parkinson A (2015b) Further characterization of the metabolism of desloratadine and its cytochrome P450 and UDP-glucuronosyltransferase inhibition potential: identification of desloratadine as a relatively selective UGT2B10 inhibitor. *Drug Metab Dispos* 43:1294–1302.

Kerdpin O, Mackenzie PI, Bowalgaha K, Finel M, and Miners JO (2009) Influence of N-terminal domain histidine and proline residues on the substrate selectivities of human UDP-glucuronosyltransferase 1A1, 1A6, 1A9, 2B7, and 2B10. *Drug Metab Dispos* 37:1948–1955.

Kiang TK, Ensom MH, and Chang TK (2005) UDP-glucuronosyltransferases and clinical drug interactions. *Pharmacol Ther* 106:97–132.

Kilford PJ, Stringer R, Sohal B, Houston JB, and Galetin A (2009) Prediction of drug clearance by glucuronidation from in vitro data: use of combined cytochrome P450 and UDP-glucuronosyltransferase cofactors in alamethicin-activated human liver microsomes. *Drug Metab Dispos* 37:82–89.

Kristensen CB, Gram LF, and Kragh-Sørensen P (1985) Mianserin protein binding in serum and plasma from healthy subjects and patients with depression and rheumatoid arthritis. *Psychopharmacology* 87:204–206.

Kubota T, Lewis BC, Elliot DJ, Mackenzie PI, and Miners JO (2007) Critical roles of residues 36 and 40 in the phenol and tertiary amine aglycone substrate selectivities of UDP-glucuronosyltransferases 1A3 and 1A4. *Mol Pharmacol* 72:1054–1062.

Kuehl GE and Murphy SE (2003) N-glucuronidation of nicotine and cotinine by human liver microsomes and heterologously expressed UDP-glucuronosyltransferases. *Drug Metab Dispos* 31:1361–1368.

Kukes VG, Kondratenko SN, Savelyeva MI, Starodubtsev AK, and Gneushev ET (2009) Experimental and clinical pharmacokinetics of amitryptiline: comparative analysis. *Bull Exp Biol Med* 147:434–437.

Lewis BC, Mackenzie PI, Elliot DJ, Burchell B, Bhasker CR, and Miners JO (2007) Amino terminal domains of human UDP-glucuronosyltransferases (UGT) 2B7 and 2B15 associated with substrate selectivity and autoactivation. *Biochem Pharmacol* 73:1463–1473.

Mackenzie PI, Bock KW, Burchell B, Guillemette C, Ikushiro S, Iyanagi T, Miners JO, Owens IS, and Nebert DW (2005) Nomenclature update for the mammalian UDP glycosyltransferase (UGT) gene superfamily. *Pharmacogenet Genomics* 15:677–685.

Manevski N, Moreolo PS, Yli-Kauhaluoma J, and Finel M (2011) Bovine serum albumin decreases K_m values of human UDP-glucuronosyltransferases 1A9 and 2B7 and increases V_{max} values of UGT1A9. *Drug Metab Dispos* 39:2117–2129.

Manevski N, Troberg J, Svaluto-Moreolo P, Dziedzic K, Yli-Kauhaluoma J, and Finel M (2013) Albumin stimulates the activity of the human UDP-glucuronosyltransferases 1A7, 1A8, 1A10, 2A1 and 2B15, but the effects are enzyme and substrate dependent. *PLoS One* 8:e54767.

Miners JO and Mackenzie PI (1991) Drug glucuronidation in humans. *Pharmacol Ther* 51:347–369.

Miners JO, Smith PA, Sorich MJ, McKinnon RA, and Mackenzie PI (2004) Predicting human drug glucuronidation parameters: application of in vitro and in silico modeling approaches. *Annu Rev Pharmacol Toxicol* 44:1–25.

Miners JO, Mackenzie PI, and Knights KM (2010a) The prediction of drug-glucuronidation parameters in humans: UDP-glucuronosyltransferase enzyme-selective substrate and inhibitor probes for reaction phenotyping and in vitro-in vivo extrapolation of drug clearance and drug-drug interaction potential. *Drug Metab Rev* 42:196–208.

Miners JO, Polasek TM, Mackenzie PI, and Knights KM (2010b) The in vitro characterization of inhibitory drug-drug interactions involving UDP-glucuronosyltransferase, in *Enzyme and Transporter Based Drug-Drug Interactions* (Pang KS, Rodrigues AD, and Peter R eds) pp 217–236, Springer, New York.

Miners JO, Bowalgaha K, Elliot DJ, Baranczewski P, and Knights KM (2011) Characterization of niflumic acid as a selective inhibitor of human liver microsomal UDP-glucuronosyltransferase 1A9: application to the reaction phenotyping of acetaminophen glucuronidation. *Drug Metab Dispos* 39:644–652.

Munro SL, Craik DJ, and Andrews PR (1987) Conformational analysis of flexible antidepressant drugs. *Quant Struct-Act Relat* 6:104–110.

Nakajima M, Tanaka E, Kwon J-T, and Yokoi T (2002) Characterization of nicotine and cotinine N-glucuronidations in human liver microsomes. *Drug Metab Dispos* 30:1484–1490.

Nakajima M and Yokoi T (2005) Interindividual variability in nicotine metabolism: C-oxidation and glucuronidation. *Drug Metab Pharmacokinet* 20:227–235.

Pattanawongsa A, Chau N, Rowland A, and Miners JO (2015) Inhibition of human UDP-glucuronosyltransferase enzymes by canagliflozin and dapagliflozin: implications for drug-drug interactions. *Drug Metab Dispos* 43:1468–1476.

Raungrut P, Uchaipichat V, Elliot DJ, Janchawee B, Somogyi AA, and Miners JO (2010) In vitro-in vivo extrapolation predicts drug-drug interactions arising from inhibition of codeine glucuronidation by dextropropoxyphene, fluconazole, ketoconazole, and methadone in humans. *J Pharmacol Exp Ther* 334:609–618.

Rowland A, Elliot DJ, Williams JA, Mackenzie PI, Dickinson RG, and Miners JO (2006) In vitro characterization of lamotrigine N2-glucuronidation and the lamotrigine-valproic acid interaction. *Drug Metab Dispos* 34:1055–1062.

Rowland A, Gaganis P, Elliot DJ, Mackenzie PI, Knights KM, and Miners JO (2007) Binding of inhibitory fatty acids is responsible for the enhancement of UDP-glucuronosyltransferase 2B7 activity by albumin: implications for in vitro-in vivo extrapolation. *J Pharmacol Exp Ther* 321:137–147.

Rowland A, Knights KM, Mackenzie PI, and Miners JO (2008) The "albumin effect" and drug glucuronidation: bovine serum albumin and fatty acid-free human serum albumin enhance the glucuronidation of UDP-glucuronosyltransferase (UGT) 1A9 substrates but not UGT1A1 and UGT1A6 activities. *Drug Metab Dispos* **36**:1056–1062.

Rowland A, Miners JO, and Mackenzie PI (2013) The UDP-glucuronosyltransferases: their role in drug metabolism and detoxification. *Int J Biochem Cell Biol* **45**:1121–1132.

Takeda S, Kitajima Y, Ishii Y, Nishimura Y, Mackenzie PI, Oguri K, and Yamada H (2006) Inhibition of UDP-glucuronosyltransferase 2b7-catalyzed morphine glucuronidation by keto-conazole: dual mechanisms involving a novel noncompetitive mode. *Drug Metab Dispos* **34**: 1277–1282.

Uchaipichat V, Mackenzie PI, Guo X-H, Gardner-Stephen D, Galetin A, Houston JB, and Miners JO (2004) Human udp-glucuronosyltransferases: isoform selectivity and kinetics of 4-methylumbelliferone and 1-naphthol glucuronidation, effects of organic solvents, and inhibition by diclofenac and probenecid. *Drug Metab Dispos* **32**: 413–423.

Uchaipichat V, Mackenzie PI, Elliot DJ, and Miners JO (2006a) Selectivity of substrate (tri-fluoperazine) and inhibitor (amitriptyline, androsterone, canrenoic acid, hecogenin, phenylbuta-zone, quinidine, quinine, and sulfinpyrazone) "probes" for human udp-glucuronosyltransferases. *Drug Metab Dispos* **34**:449–456.

Uchaipichat V, Winner LK, Mackenzie PI, Elliot DJ, Williams JA, and Miners JO (2006b) Quantitative prediction of in vivo inhibitory interactions involving glucuronidated drugs from in vitro data: the effect of fluconazole on zidovudine glucuronidation. *Br J Clin Pharmacol* **61**:427–439.

Virtanen R, Scheinin M, and Iisalo E (1980) Single dose pharmacokinetics of doxepin in healthy volunteers. *Acta Pharmacol Toxicol* **47**:371–376.

Walsky RL, Bauman JN, Bourcier K, Giddens G, Lapham K, Negahban A, Ryder TF, Obach RS, Hyland R, and Goosen TC (2012) Optimized assays for human UDP-glucuronosyltransferase (UGT) activities: altered alamethicin concentration and utility to screen for UGT inhibitors. *Drug Metab Dispos* **40**:1051–1065.

Zhou D, Guo J, Linnenbach AJ, Booth-Genthe CL, and Grimm SW (2010) Role of human UGT2B10 in N-glucuronidation of tricyclic antidepressants, amitriptyline, imipramine, clo-mipramine, and trimipramine. *Drug Metab Dispos* **38**:863–870.

Address correspondence to: Dr. John O. Miners, Department of Clinical Pharmacology, School of Medicine, Flinders University, GPO Box 2100, Adelaide, SA 5001, Australia. E-mail: john.miners@flinders.edu.au